Neuropsychopharmacology (2008) 33, 2442–2455

www.neuropsychopharmacology.org

Postnatal Phencyclidine Administration Selectively Reduces Adult Cortical Parvalbumin-Containing Interneurons

Cheng Z Wang[1], San F Yang[1], Yan Xia[1] and Kenneth M Johnson*[,1,2]

[1]Department of Pharmacology and Toxicology, University of Texas Medical Branch, Galveston, TX, USA; [2]Center for Addiction Research, University of Texas Medical Branch, Galveston, TX, USA

Transient postnatal NMDA receptor blockade by phencyclidine (PCP), ketamine, or MK-801 induces developmental neuroapoptosis and adult behavioral deficits, which resemble abnormal human behaviors typically present in schizophrenia. This study tested the hypothesis that PCP-induced developmental apoptosis causes a specific deficit of GABAergic interneurons containing parvalbumin (PV), calretinin (CR), or calbindin (CB). Young adult (PND56) rats that were given a single dose of PCP (10 mg/kg) on PND7 exhibited no densitometric change of either CR or CB neurons in any brain region studied, but demonstrated a selective deficit of PV-containing neurons in the superficial layers (II–IV) of the primary somatosensory (S1), motor (M), and retrosplenial cortices, but not in the striatum (CPu) or hippocampus. Further, CR and CB neurons, which were expressed at the time of PCP administration, showed no colocalization with cellular markers of apoptosis (terminal dUTP nick-end labeling (TUNEL) of broken DNA or cleaved caspase-3), indicating that CR- and CB-containing neurons were protected from the toxic effect of PCP and survived into adulthood. This suggests that the deletion of PV neurons occurred during development, but cleaved caspase-3 showed no colocalization with BrdU, a specific marker of S-phase proliferation. These data suggest that the loss of PV-containing neurons was not due to an effect of PCP on proliferating neurons, but rather an effect on post-mitotic neurons. The developmental dependence and neuronal specificity of this effect of PCP provides further evidence that this model may be valuable in exploring the pathophysiology of schizophrenia.
Neuropsychopharmacology (2008) **33,** 2442–2455; doi:10.1038/sj.npp.1301647; published online 5 December 2007

Keywords: phencyclidine; parvalbumin; schizophrenia; neuroapoptosis; neurogenesis; *N*-methyl-D-aspartate receptor

INTRODUCTION

Schizophrenia affects approximately 1% of the world's population and causes a lifelong disability for most victims. Schizophrenia is also a severe emotional and economic burden for both patients and their families (Lewis and Gonzalez-Burgos, 2006). Unfortunately, its etiology and pathophysiology are poorly defined. Nevertheless, accumulating literature, including several meta-analyses, strongly suggests that there is a neuropathology of schizophrenia (Harrison and Weinberger, 2005), which include enlargement of ventricles and volumetric reductions in whole brain (Lawrie and Abukmeil, 1998; Wright *et al*, 2000) as well as specific brain regions, such as the hippocampus (Nelson *et al*, 1998; Heckers, 2001), association neocortex (prefrontal (PFC) and superior temporal) (Pearlson and Marsh, 1999; Shenton *et al*, 2001; Davidson and Heinrichs, 2003), and thalamus (Konick and Friedman, 2001). Histological findings include cytoarchitectural abnormalities such as aberrant invaginations of the surface, disruption of cortical layers, heterotopic displacement of neurons, and paucity of neurons in superficial layers (II–IV) of the entorhinal cortex (Jakob and Beckmann, 1986; Arnold *et al*, 1991; Falkai *et al*, 2000; Kovalenko *et al*, 2004). Further, significant reduction of GABAergic interneurons (small, nonpyramidal) has been reported in layer II of anterior cingulate (ACC) and PFC cortices (Benes *et al*, 1991, 2001; Benes and Berretta, 2001) as well as hippocampus (Benes *et al*, 1998) of schizophrenic brains. GABAergic interneurons containing parvalbumin (PV), a calcium-binding protein (CBP) were found decreased in superficial cortical layers (III and IV) of PFC (Beasley and Reynolds, 1997; Lewis, 2000; Reynolds *et al*, 2002).

1-(1-Phenylcyclohexyl) piperidine (phencyclidine or PCP) has long been recognized to induce negative and positive symptoms of schizophrenia in normal humans (Luby *et al*, 1959; Javitt and Zukin, 1991). More recent reports demonstrated that acute postnatal administration of NMDA receptor antagonists (including PCP, ketamine, and MK801) induced robust and widespread neuroapoptosis during brain development in rodents (Ikonomidou *et al*, 1999; Scallet *et al*, 2004; Young *et al*, 2005; Wang and Johnson, 2005, 2007). Importantly, early postnatal acute administration of NMDA receptor antagonists produces behavioral deficits in adulthood, which resemble behavioral

*Correspondence: Dr KM Johnson or Dr CZ Wang, Department of Pharmacology and Toxicology, University of Texas Medical Branch, 301 University Blvd, Galveston, TX 77555-1031, USA, Tel: +1 409 772 9623, Fax: +1 409 772 9642, E-mails: kmjohnso@utmb.edu or czwang@utmb.edu
Received 17 September 2007; revised 25 October 2007; accepted 27 October 2007

abnormalities typically present in schizophrenia (Harris *et al*, 2003; Fredriksson and Archer, 2003, 2004; Fredriksson *et al*, 2004; Wozniak *et al*, 2004). For example, acute treatment of mice with MK801, ketamine, or ethanol at postnatal day (PND) 10 or PND11 showed marked and lasting hyperactivity at PND60, as well as a deficit in acquisitive performance in the radial arm maze test and a deficit in circular swim maze test (Fredriksson and Archer, 2004), each of which are mouse behaviors postulated to be of potential relevance to signs and symptoms of schizophrenia (Powell and Miyakawa, 2006). Interestingly, administration of NMDA receptor antagonists to developing rodents resulted in the death of neurons in brain regions similar to the neuropathology observed in post-mortem brains from patients with schizophrenia (Ikonomidou *et al*, 1999; Wang and Johnson, 2005, 2007).

These results prompted us to propose that PCP-induced developmental apoptosis might lead to neuronal deficits in adult brain similar to the neuropathology found in schizophrenic brain. The present study used immunohistochemical (IHC) peroxidase staining, unbiased IHC image analysis, and IHC-multifluorescent (MFL) labeling to investigate whether PCP-induced developmental neuroapoptosis results in a specific deficit of GABAergic interneuron populations including those containing either PV, calretinin (CR), or calbindin (CB) in adulthood. We also determined whether PCP targets progenitor cells during brain development.

MATERIALS AND METHODS

Experimental Paradigms and Brain Sample Processing

An equal number of male and female PND 7 rat pups were subcutaneously (s.c.) injected with a single dose of either saline (control) or PCP. Afterward, they were subjected to one of the three experimental protocols: (1) killed at PND56 to define the effects of postnatal PCP administration on adult expression of GABAergic interneuron subpopulations, (2) killed 9 h later to determine whether PCP targeted CR and CB, and (3) killed 9 h after administration of PCP and BrdU to define the relationship between PCP-induced developmental neuroapoptosis and postnatal neurogenesis.

Timed pregnant Sprague–Dawley rats (Charles River Laboratories, Inc. Wilmington, MA, USA) were received on embryonic day 14 (E14, with the day after breeding considered E0) and housed individually with a 12 h light–dark cycle (lights on at 0700 hours, off at 1900 hours) in a temperature- and humidity-controlled environment with free access to food and water. On PND2 (E21 was set up as PND0), pups were culled to four of each gender to ensure an equal number of both sexes in each litter. On PND7, the pups were randomly assigned to either the saline or PCP group (each of which contained an equal number of each gender), and s.c. injected with a single dose of either saline (10 ml/kg) or PCP (10 mg/kg, acquired from the National Institute on Drug Abuse, Rockville, MD, USA), and thereafter returned to their mothers. For those rats used for IHC detection at PND56, pups were weaned on PND22, separated into groups of four pups per single-sex cage, and housed until the end of the experiment.

The processing of brain samples has been detailed elsewhere (Wang and Johnson, 2005, 2007). Briefly, at either PND56 or PND7, rats were deeply anesthetized with 100 mg/kg pentobarbital sodium and perfused through the left ventricle and ascending aorta with ice-cold heparinized (10 U/ml) phosphate-buffered saline (PBS, 0.01 M, pH 7.4) followed by ice-cold 4% paraformaldehyde in PBS. The perfused brain was postfixed by immersion in the same fixative for 24 h for IHC and terminal dUTP nick-end labeling (TUNEL) staining or for at least 2 days for silver staining before sectioning. The left hemisphere from each brain was serially cut on a Vibratome into 50 μm-thick sagittal sections, which were subsequently used to identify the anteroventral thalamic nucleus (AV), hippocampal CA1, dorsal subiculum (DS), and retrosplenial cortex (RSC). The right hemisphere was serially cut into 50 μm-thick coronal sections and was subsequently used to define the lateral extent of the striatum (CPu) and the cingulate (Cg), motor (M), and anterior primary somatosensory (S1) cortices. Brain atlases for both developing (Sherwood and Timiras, 1970; Paxinos *et al*, 1994) and adult rats (Paxinos and Watson, 2007) were used as guides to identify these regions. According to the principles of unbiased, systematic random sampling (West, 1993), 30 serial sections were transferred into one of six wells, with every sixth section being placed in the same well with antifreeze solution and kept at -20°C for future processing.

IHC Peroxidase Staining and Cupric Silver Staining

As previously described, neurons containing CBP PV (Solbach and Celio, 1991), CR (Gritti *et al*, 2003), or CB (Alcántara *et al*, 1993) were immunolabeled by using the ABC peroxidase system. Briefly, free-floating sections removed from antifreeze solution were washed with TBS (0.1 M, pH 7.4), pretreated with Triton X-100 (0.4% in TBS for 6 h at 4°C), quenched for 10 min in 3% hydrogen peroxide/methanol, blocked for 1 h with 2% BSA, 10% normal goat serum, 0.2% milk, 0.1 M TBS and incubated for 72 h at 4°C with mouse monoclonal IgG1 against PV (clone PARV-19; 1:1000, no. P-3088, Sigma Chemicals, St Louis, MO, USA), or rabbit IgG against CR (a synthetic peptide corresponding to the C-terminal region of rat CR (aa 194–209) conjugated to KLH; 1:1000, no. C-7479, Sigma), or rabbit IgG against CB-D-28 (EG-20; a synthetic peptide corresponding to the C-terminal region of rat CB-D-28 (aa 225–244 with N-terminally added Lys-Gly) conjugated to KLH; 1:1000, no. C-2724, Sigma). After washes with TBS, the sections were incubated for 90 min with biotinylated goat anti-mouse (for PV) or goat anti-rabbit (for both CR and CB) antibodies (Vector Laboratories, Burlingame, CA, USA), reacted in the dark for 1 h with ABC reagents (standard Vectastain ABC Elite Kit; Vector Laboratories), and developed with a filtered mixture of Vector SG substrate (gray; Vector Laboratories).

Neuronal degeneration was determined as previously described (Carlsen and De Olmos, 1981; Wang and Johnson, 2005). Nissl staining and toluidine blue staining were used to demonstrate normal brain morphology and in turn to guide the identification of brain regions of interest.

Quantitative Image Analysis

Immunolabeled PV, CR, and CB neurons were quantified on photomicrographs of the following brain regions as guided

by using atlases for adult rats (Paxinos and Watson, 2007): Cg, M and S1, and CPu, figures 16–30; CA1, DS, and RSC, figures 167–173. The photomicrographs of each region were taken through a $\times 10$ objective using a Hammatsu digital camera (C4742-95) based on the demarcations previously defined (Wang and Johnson, 2007).

As previously described (Wang and Johnson, 2007), the quantification was carried out by automatically measuring the number of positive neurons in a defined area of interest (AOI) within the photomicrographs of each brain region by using a computer-based image analysis program, SimplePCI (Compix Inc. Imaging Systems, Cranberry Township, PA, USA). The program converted all AOI thus defined automatically from pixels to μm^2 based on calibration files. The number of positive cells was estimated by using a double threshold technique based on boundary metrics for average neuronal size and gray level, in which two operators agreed that a gray range setting, along with the size discriminator, accurately counted the number of positive neurons. The gray level ranges were set up as follows: 0–100 for PV-positive neurons, 0–127 for CR, and 0–60 for CB. Neuronal area sizes were set up to range between 28 μm^2 ($\sim$6 μm diameter) and 250 μm^2 ($\sim$18 μm diameter) for all three subpopulations. The average value from all five sections taken from each region was used to represent the regional value for each animal.

IHC-MFL of Apoptotic Markers and CR or CB

Triple labeling of TUNEL, CR or CB, and NeuN or GFAP was carried out in the following order: single labeling of TUNEL followed by double labeling of CR or CB and NeuN or GFAP. TUNEL was carried out by the aid of deoxynucleotidyl transferase (200 U/ml) and biotin-16-dUTP (10 nmol/ml) purchased from Roche Diagnostics (Indianapolis, IN, USA), and incorporated biotin-16-dUTP was visualized by using Streptavidin Alexa Fluor 594 conjugate (1:200 of 2 mg/ml, Invitrogen Corporation, Carlsbad, CA, USA) (Wang and Johnson, 2007). The sections were then labeled with CR or CB and NeuN or GFAP by following the protocols of the ABC peroxidase system as described except that the quenching of endogenous peroxidase was omitted. The sections were incubated with primary rabbit antibodies against CR or CB for 48 h at 4°C, and then with primary monoclonal antibodies against NeuN or GFAP (both 1:500, Chemicon International, Temecula, CA, USA) for another 24 h. After washing with 0.1 M TBS, the sections were incubated with a mixture of goat anti-rabbit IgG (Alexa Fluor 488 conjugate, Invitrogen; 1:200) and goat anti-mouse IgG (Alexa Fluor 633 conjugate, Invitrogen; 1:200) for 60 min in the dark.

For double labeling of cleaved caspase-3 and CR, CR labeling with goat anti-rabbit IgG (Alexa Fluor 488 conjugate, Invitrogen) was carried out as above except that the quenching of endogenous peroxidase was omitted. The sections were then treated with 0.4% Triton X-100 for 1 h followed by the labeling of cleaved caspase-3 with primary rabbit antibodies against cleaved caspase-3 (Asp175; 1:1000, no. 9661, Cell Signaling Technology, Danvers, MA, USA) and goat anti-rabbit IgG (Alexa Fluor 594 conjugate, Invitrogen; 1:200) (Wang and Johnson, 2007).

Specimens were visualized using a Zeiss LSM510 META confocal system configured with a Zeiss Axiovert 200 M motorized inverted microscope. All images were acquired using a C-Apochromat $\times 40$ (1.2 NA) water-immersion objective lens and the scanning zoom was adjusted for optimal space sampling (pixel size 110×110 nm). Multi-labeled fluorescent samples were imaged acquiring each fluorescent channel sequentially to avoid signal bleedover. The Alexa 488 component was obtained using the 488 nm line of an argon ion laser for excitation and a band pass (505–530 nm) emission filter. The Alexa 594 component was obtained using the 543 nm line of a green helium/neon laser for excitation and a band-pass (585–615 nm) emission filter. Images were visualized and processed by using the Zeiss Image Browser freeware program.

BrdU *In Vivo* Incorporation and IHC-MFL of BrdU and Cleaved Caspase-3

Just prior to the administration of saline or PCP (10 mg/kg, s.c.), PND7 rat pups were s.c. injected with BrdU (50 mg/kg, $2\times$, 4.5 h apart; Roche Diagnostics), and killed for brain sampling 9 h later. The survival time interval (9 h after PCP and BrdU) was based on two considerations: (1) it is near the peak time of the apoptotic response to PCP (Wang and Johnson, 2005) and (2) it is within one cell cycle. Thus, the detected proliferation in the present study did not include progeny of previously labeled cells. Following either i.p. or i.v. administration BrdU is transported across the blood–brain barrier by the thymidine nucleoside transporter (Lynch *et al*, 1977) and is metabolized rapidly through dehalogenation with a half-life of approximately 10 min (Kriss *et al*, 1963) and may also be eliminated through the cerebrospinal fluid (Thomas née Williams and Segal, 1996; Thomas *et al*, 1997; Spector and Berlinger, 1982). The S phase of a cell cycle is about 6–7 h and a cell cycle has been estimated at 12–14 h (Hayes and Nowakowski, 2002) as the S phase commonly comprises a third to half of the cell cycle (Alexiades and Cepko, 1996; Bhide, 1996; Takahashi *et al*, 1995). The BrdU dose and injection interval chosen were based in part on the distribution and clearance rate demonstrated by others (Packard *et al*, 1973; Hayes and Nowakowski, 2000) as well as studies showing that the chosen dose that labels every cell in the S phase in the region of the cortical ventricular zone of embryonic mice without apparent toxic effects (Miller and Nowakowski, 1988; Takahashi *et al*, 1992; Taupin, 2007). BrdU was s.c. injected using a modification of an osmotic pump method (Eldridge *et al*, 1990). Preliminary experiments showed that multiple injections (50 mg/kg, s.c., every 2, 3, or 4.5 h) showed as much as twice the labeling as a single injection, but the interval between injections did not have a marked effect on BrdU labeling.

IHC-MFL of BrdU and cleaved caspase-3 was carried out as previously described (Komitova *et al*, 2002). After washing with 0.01 M PBS, sections were treated in 2 M HCl at 37°C for 30 min, rinsed in borate buffer (pH 8.5), washed in TBS (0.08 M Trizma-HCl, 0.016 M Trizma-Base, 0.15 M NaCl, pH 7.5), and finally with 0.01 M PBS for 10 min each (Palmer *et al*, 2000). The sections were blocked for 1 h with blocking solution (2% BSA, 10% normal goat serum, 0.2% milk, 0.3% Triton X-100 in 0.01 PBS), after which a mixture of mouse anti-BrdU (Roche or Sigma, 1:200) and rabbit anti-cleaved caspase-3 (Asp175) antibodies was added

(1:500, Cell Signaling Technology), and then incubated overnight at 4°C with agitation. After washes with 0.01 M PBS, the sections were incubated for 90 min with goat anti-mouse IgG (Alexa Fluor 594 or 488 conjugate, 1:200, Invitrogen) and goat anti-rabbit IgG (Alexa Fluor 488 or 594 conjugate, 1:200, Invitrogen).

Statistical analysis. All the experimental data are presented as the mean ± SE. Unpaired *t*-tests (two-tailed) were used to determine differences between two groups. Differences were considered significant at $p < 0.05$.

RESULTS

Quantitative Image Analysis of CBP-Containing Neurons

To test the hypothesis that PCP-induced developmental neuroapoptosis leads to a deficit of GABAergic interneuron subpopulations in adulthood, we administrated PCP to PND7 rat pups and quantitated the expression of PV, CR, and CB neurons on PND56. We chose PND7 to inject PCP because it has been reported to be the age most susceptible to the apoptotic effect of PCP or MK801 treatment (Ikonomidou *et al*, 1999; Wang and Johnson, 2005). We selected the S1, M, RSC, Cg, CA1, Cpu, and DS to quantitatively analyze the densities of PV, CR, and CB neurons based on our previous findings that these were the brain regions most vulnerable to the apoptotic effects of acute phencyclidine administration during brain development (Wang and Johnson, 2005, 2007). Although the AV was also targeted by PCP as evidenced by positive silver staining after PCP treatment at PND7 (Figure 1a), this region was not included in this analysis because it did not contain any neurons expressing PV, CR, or CB during development (Figure 1b; CB, PND7 normal rat) or in young adults (Figure 1c, CR, PND56 rat after saline treatment at PND7; Figure 1d, PV, PND56 rat with PCP injection at PND7).

PV neurons were expressed in all brain regions studied in PND56 rats that were injected with saline or PCP (10 mg/kg, s.c.) on PND7. PV was quantified in all regions except the DS due to its very low density. As shown in Table 1, the number of PV neurons in PCP-treated animals was significantly reduced by 64% in S1, 36% in M, and 21% in RSC ($p < 0.05$). In these cortical regions, the reduction was limited to superficial layers 2–4 as evidenced in the S1 cortex (Figure 2) as well as in the M (Figure 3), while the deep layers (5–6) showed no significant difference between saline and PCP treated brains as shown in the M (Figure 3). In the cingulate cortex and hippocampal CA1 region, the number of PV-positive neurons in PCP-treated rats were 90 and 91% of saline controls, respectively, but this modest trend toward a decrease was not significant ($p > 0.05$). In the striatum, the number of PV-positive neurons in PCP-treated animals was 96% of saline controls ($p > 0.05$). Despite the

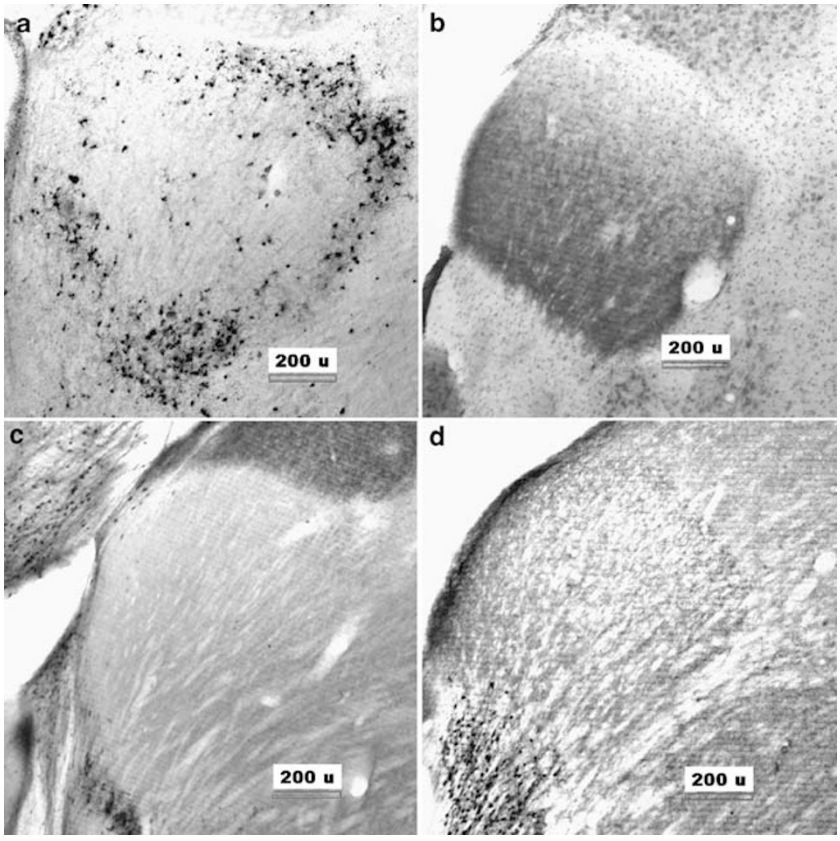

Figure 1 Representative microphotographs of anteroventral (AV) thalamic nucleus showing: (a) positive silver-staining neurons 16 h after PCP treatment (10 mg/kg, s.c.) at PND7; (b–d), negative expression of CBPs-containing neurons during development and in adults. (b) Normal PND7 rat pups showed absence of CB neurons. (c) PND56 rats showed no CR neurons after saline treatment at PND7. (d) PND56 rats showed no PV neurons after PCP (10 mg/kg, s.c.) injection at PND7. Scale bars = 200 μm.

Table 1 Expression of CBPs-Containing Neurons in Brains of Young Adult Rats Injected with Single Dose of Phencyclidine (10 mg/kg) on PND7

		Positive CBPs-containing neurons per mm^2 in several brain regions						
CBPs	**Treatment**	**S1**	**M**	**RSC**	**Cg**	**CA1**	**CPu**	**DS**
PV	Saline	121 ± 23	177 ± 20	234 ± 21	261 ± 15	104 ± 7	55 ± 5	ND[a]
	PCP	44 ± 6*	113 ± 16*	185 ± 7*	236 ± 17	94 ± 5	53 ± 4	ND[a]
	Change (%)[b]	(36)	(64)	(79)	(90)	(91)	(96)	NA[c]
CR	Saline	39 ± 4	51 ± 7	121 ± 12	119 ± 6	28 ± 1	5 ± 1	115 ± 5
	PCP	39 ± 3	56 ± 6	116 ± 3	108 ± 7	28 ± 2	6 ± 1	103 ± 8
	Change (%)[b]	(99)	(109)	(96)	(91)	(100)	(109)	(90)
CB	Saline	169 ± 7	84 ± 22	37 ± 7	45 ± 8	37 ± 5	nd[d]	ND[a]
	PCP	161 ± 27	88 ± 23	33 ± 6	43 ± 9	40 ± 13	nd[d]	ND[a]
	Change (%)[b]	(95)	(105)	(91)	(97)	(108)	NA[c]	NA[c]

Abbreviations: CBPs, calcium-binding proteins; PV, parvalbumin; CR, calretinin; CB, calbindin; PCP, phencyclidine; S1, primary somatosensory cortex; M, motor cortex; RSC, retrosplenial cortex; Cg, cingulate cortex; CA1, hippocampal CA1 subregion; CPu, caudate putamen; DS, dorsal subiculum.
*$p < 0.05$ *vs* corresponding saline value (unpaired *t*-test, two-tailed).
[a]ND, not determined.
[b]Change, percentage of regional corresponding saline control.
[c]NA, not available.
[d]nd, not detectable.

lack of effect on the number of PV-positive neurons in the striatum, the number and extent of dendritic branches of PV neurons appeared to be significantly reduced by PCP treatment (Figure 4a, saline; Figure 4b, PCP), though this was not quantified.

CR-positive neurons were localized in all seven brain regions studied (Table 1) with very low density in lateral striatum (CPu), but a high density in the DS (Figure 5) compared to that of PV or CB in the same region (Table 1). Therefore, the DS was added to evaluate the CR density after PCP treatment. PCP had no significant effect on the number of CR-positive neurons in either S1, M RSC, Cg, CA1, CPu, or DS (Figure 5a and b). Further, there was no consistent trend toward either an increase or decrease when considered as a whole.

CB neurons were quantified in five of the brain regions studied. As shown in Table 1, PCP treatment had no significant effect on the density of CB neurons in any of the five areas examined ($p > 0.05$, Table 1). Further, there was no trend toward either an increase or decrease when the five brain regions were considered as a whole. It should also be noted that CB containing neurons were not detectable in the CPu and the density found in the DS was too low and variable to accurately quantify. Thus, CB- and CR-containing interneurons may be absolutely invulnerable to the apoptotic effect of PCP.

Colocalization of Apoptotic Markers and CR or CB

To further test the hypothesis that CR and CB neurons are not apoptotic targets of PCP during brain development, we injected 10 mg/kg PCP to PND7 rat pups and determined whether apoptotic markers (TUNEL or cleaved caspase-3) were colocalized with either CR or CB in neurons 9 h following administration. This paradigm was chosen as we had previously shown co-expression of TUNEL and cleaved caspase-3 in the same neurons in PND7 rats after PCP administration (Wang and Johnson, 2007). Although PCP did cause significant neurodegeneration in the DS in PND7 rat pups 16 h after injection (Figure 5c), IHC-MFL failed to show colocalization of TUNEL-positive nuclei in any CB-positive neurons (data not shown) or in the majority of CR-positive neurons (Figure 5d), suggesting that these markers are labeling different cell populations. However, we did observe one CR-positive neuron that was colocalized in a cell with a TUNEL-positive nucleus. This may be representative of the insignificant effect of PCP on CR neurons in the DS observed in adults (Table 1). As represented in Figure 6, IHC-MFL failed to colocalize the apoptotic markers (TUNEL or cleaved caspase-3) with either CR or CB in all other brain regions studied, including M (CR, Figure 6a), Cg (CR, Figure 6b), S1 (CR, Figure 6c; CB, Figure 6f), CA1 (CR, Figure 6c; CB, Figure 6d), RSC (data not shown), and CPu (data not shown).

Colocalization of Cleaved Caspase-3 and BrdU

Since PCP selectively affected PV-containing neurons over those containing CR or CB, we postulated that this selectivity may in part be due to the fact that expression of CB and CR was already evident at the time of administration, while PV had yet to be expressed by PND7. One possible explanation for the selectivity of PCP in this regard may have to do with maturity of the neurons. That is, PCP may be more selective for immature neurons, including proliferating cells. To test this hypothesis, we injected BrdU immediately before PCP administration to label rapidly dividing cells and then determined the degree of

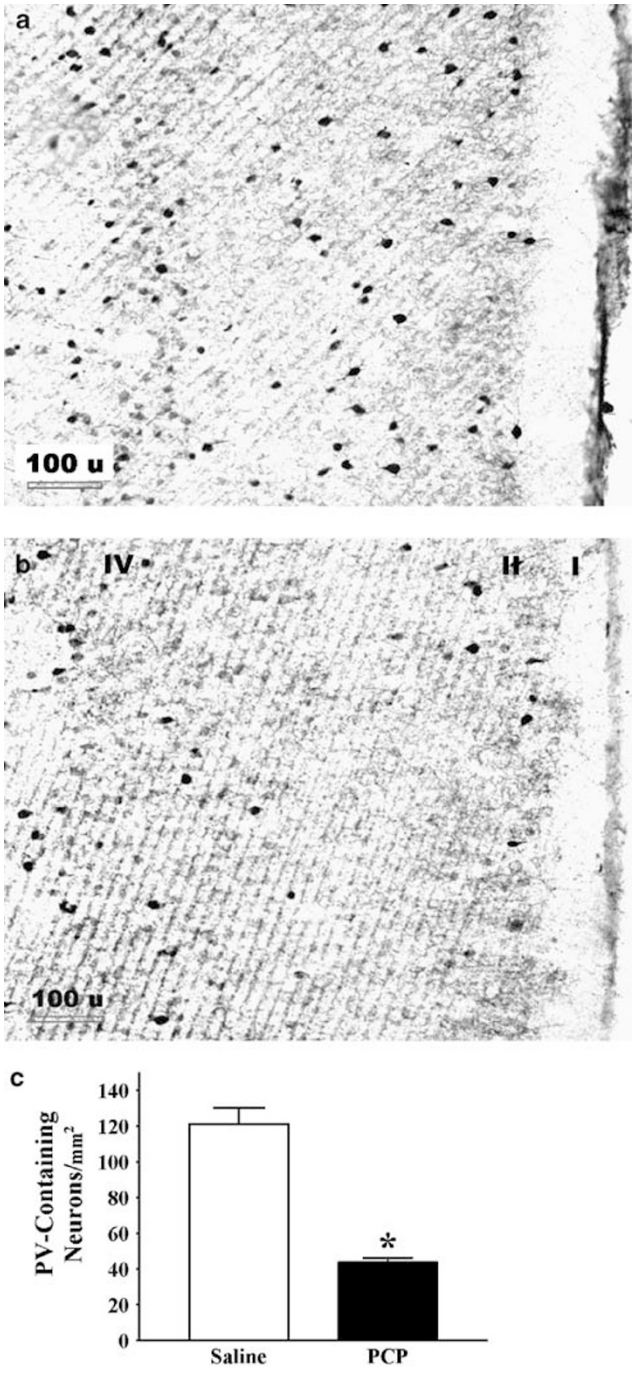

Figure 2 Representative expression of PV neurons in primary somatosensory cortex (S1) of PND56 rats treated with saline (a) or PCP (10 mg/kg, s.c.) (b) at PND7: layers 2–4 showed significantly fewer PV neurons in PCP-treated animals than saline-treated rats. I, II, and IV reference S1 layers 1, 2, and 4, respectively. Scale bars = 100 μm. (c) Quantitative analysis of PV-containing neurons in S1 layers 2–4 of PND56 rats treated with saline or PCP (10 mg/kg, s.c.), showing developmental PCP administration induced significant reduction of PV neurons. Statistical analysis: unpaired *t*-test (two-tailed). *$p < 0.05$ *vs* corresponding saline value.

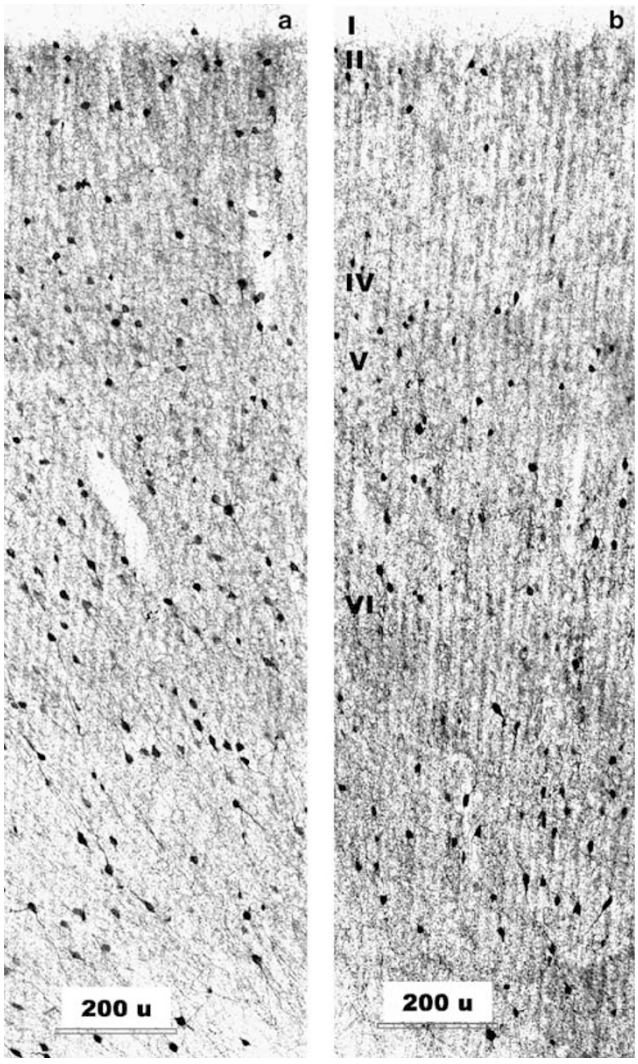

Figure 3 Representative expression of PV neurons in motor cortex (M) of PND56 rats with injection of saline (a) or PCP (10 mg/kg, s.c.) (b) at PND7: layers 2–4 showed significantly fewer PV-positive neurons in PCP-treated animals than in saline-treated rats, while deep layers (5–6) showed no difference between the two treatments. I, II, IV, V, and VI, motor cortex layers 1, 2, 4, 5, and 6, respectively. Scale bars = 200 μm.

colocalization of cleaved caspase-3 and BrdU in several brain regions 9 h later. Our preliminary studies showed that this protocol of *in vivo* BrdU incorporation (50 mg/kg, 2 ×, 4.5 h apart, s.c.) provided saturated labeling of proliferating cells (data not shown). Positive BrdU labeling was found in all brain regions and subregions studied including, but not limited to, M, S1, retrosplenial and Cg, striatum, hippocampus and thalamus of rat pups treated with both saline (data not shown), and PCP (Figure 7). In other words, all brain regions that demonstrated neuroapoptosis after PCP administration at PND7 showed cell proliferation simultaneously, indicating a possible spatial relationship between them. However, these brain regions and subregions showed no colocalization of cleaved caspase-3 and BrdU in the same neurons as shown in Figure 7, suggesting that PCP administration during this stage of development did not target proliferating neurons.

DISCUSSION

It has been previously documented that postnatal NMDA receptor blockade by PCP, MK801, and ketamine induced

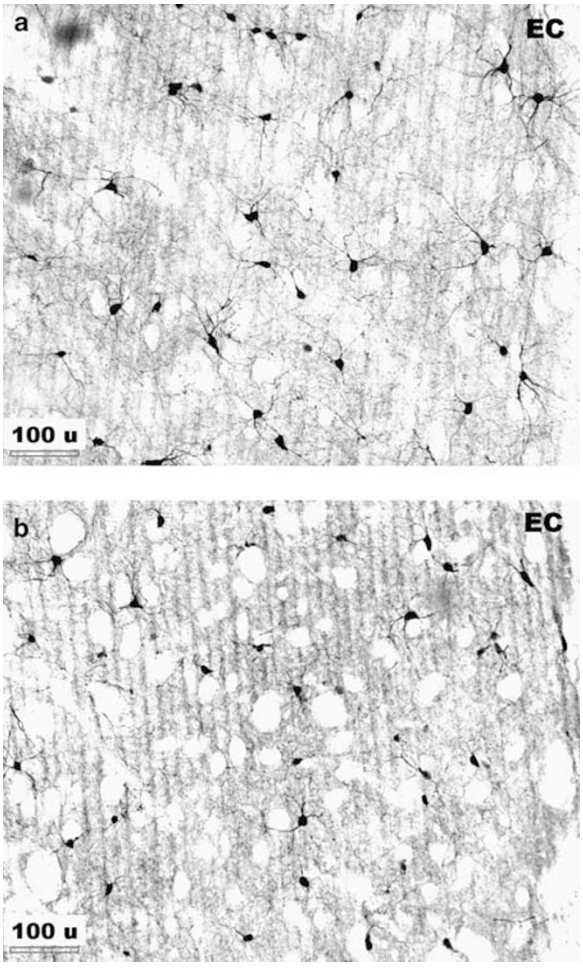

Figure 4 Representative microphotographs of the striatum (CPu) demonstrating no significant difference in the number of PV neurons found in PND56 rats injected with either saline (a) or PCP (10 mg/kg, s.c.) (b) on PND7. However, PCP substantially reduced the number of dendrites and the degree of branching of PV neurons in the CPu (b) relative to those treated with saline (a). EC, external capsule. Scale bars = 100 μm.

developmental neuroapoptosis (Ikonomidou *et al*, 1999, 2000; Olney *et al*, 2002; Scallet *et al*, 2004; Young *et al*, 2005; Wang and Johnson, 2005, 2007). However, whether this insult affects the development of specific neuronal populations in adulthood has not been addressed. This report examined the effect of acute postnatal NMDA receptor blockade on expression of GABAergic interneuron subpopulations containing PV, CR, or CB in young adult rodents (PND56). Among these interneurons, this effect was selective for PV-containing neurons. The effect on PV neurons was also largely selective for cortical regions. That is, the superficial layers (II–IV) of S1, M, and RSC of PCP-treated rats demonstrated significant reduction of PV neurons compared to saline controls, while the striatum (CPu) and hippocampus were not significantly different from controls. Interestingly, CR and CB were expressed at the time of PCP injection (PND7), but were unaffected; however, PV is not expressed at this stage and these neurons were susceptible to the toxic effect of PCP. IHC-MFL of apoptotic molecules (TUNEL or cleaved caspase-3) and CR or CB confirmed our hypothesis that CR- and CB-containing interneurons were not susceptible to NMDA receptor blockade, as evidenced by the lack of colocalization of either apoptotic marker with CR or CB. Further, IHC-MFL co-labeling of BrdU and cleaved caspase-3 did not demonstrate colocalization of these two markers, thereby failing to support the hypothesis that NMDA receptor blockade during brain development targets proliferating cells. Given that NMDA receptor blockade-induced neuroapoptosis is developmentally regulated (Ikonomidou *et al*, 1999, 2000; Olney *et al*, 2002; Wang and Johnson, 2005), the fact that BrdU labeling and PCP-induced caspase-3 activation were co-expressed in the same brain regions and the same cortical layers suggests that there may be a relationship, though currently undefined, between PCP-induced toxicity in PV-containing neurons and postnatal neurogenesis. As discussed below, it is also possible that this selective effect of PCP on PV-containing interneurons may play a role in the behavioral deficits observed in rodents following acute treatment with NMDA receptor antagonists during brain development (Harris *et al*, 2003; Fredriksson and Archer, 2003, 2004; Fredriksson *et al*, 2004; Wozniak *et al*, 2004).

Subchronic prenatal exposure (E15–E18) to MK-801 (0.2 mg/kg) has previously been reported to reduce the density of PV immunoreactive neurons in rat medial PFC cortex in young adults (PND63, Abekawa *et al*, 2007), but this effect was limited to the deep layers (5–6). This difference might be due to the different dose regimens used (acute single *vs* subchronic) and/or the age (postnatal *vs* prenatal) at the time of drug administration. The present study also differs from an earlier study by Sadikot *et al* (1998) that showed that subchronic CGS-19755 or MK-801 administered during the proliferative phase (E15–E18) showed a marked reduction of PV neuron cell density in the striatum of adolescent brains. Interestingly, when these authors administered CGS-19755 or MK-801 during the postproliferative period (E18–E21), no significant reduction in striatal PV neuron cell density was observed, thereby suggesting that PV-containing striatal neurons are sensitive to NMDA blockade in the proliferative period, but not the postproliferative period (Sadikot *et al*, 1998). In addition, the present data are somewhat at odds with a recent report on the developmental effects of ethanol, a drug that also has NMDA antagonist properties (Lovinger *et al*, 1989; Hoffman *et al*, 1989). In distinction to our finding, Granato (2006) reported that PND60 Wistar rats showed no densitometric change of PV neurons, but an increase in CR neurons and a decrease in CB neurons in M1 and S1 after ethanol inhalation from PND2 to PND6. While the exact cause of this difference is unknown, it is reasonable that the well-known pharmacological differences between ethanol and PCP (Hoffman *et al*, 1989) play a causative role. Further, ethanol has been reported to cause a fundamentally different neurotoxicity in developing rodent brains (Ikonomidou *et al*, 2000) when compared to the apoptotic effects of MK801 or PCP. For example, in cortex, MK-801 mainly targeted superficial layers, while ethanol damaged the superficial as well as the intermediate layers. In the anterior thalamus, MK-801 and ethanol both affected the laterodorsal, anteroventral, and anteromedial (AM) nuclei, but only ethanol affected the anterodorsal nucleus (Ikonomidou *et al*, 2000).

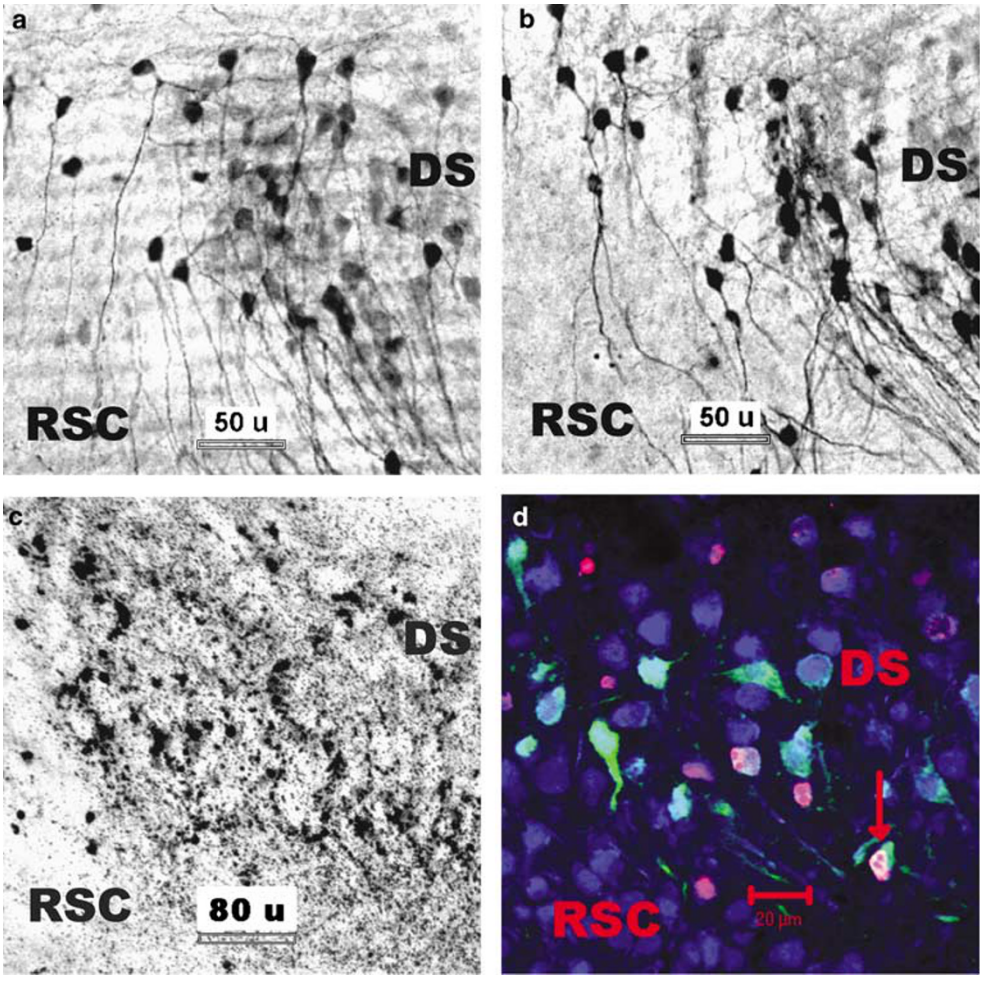

Figure 5 Representative photomicrographs of the dorsal subiculum (DS) and retrosplenial cortex (RSC) demonstrating the lack of effect of PCP on the number of CR neurons in the presence of significant PCP-induced neurotoxicity: (a, b) PND56 rats showed no significant difference in the number of CR neurons between saline (a) and PCP (10 mg/kg, s.c.) (b) administered on PND7. (c) PND7 rat pup showed extensive positive silver staining 16 h after PCP treatment (10 mg/kg, s.c.); (d) 9 h after PCP (10 mg/kg) injection, PND7 pups demonstrated that the majority of TUNEL-labeled multifragmented nuclei (red) were not co-expressed with CR (green) except one neuron (arrow), suggesting they belong to different cell populations. Blue, NeuN (a neuron-specific protein) positive staining. Scale bars = 80 μm (a), 20 μm (b), 50 μm (c, d).

Our current working hypothesis is that CBPs, including PV, CR, and CB serve to buffer both excesses and deficiencies in intracellular calcium and thus are necessary to protect developing neurons from neurotoxicity caused by PCP. In the present study, both CR and CB were expressed at the time of PCP administration and neither population showed colocalization with either apoptotic marker used (TUNEL or cleaved caspase-3). Further, there was no loss of either population in any region studied in adulthood. In contrast, PV was not expressed at the time of PCP injection, but these neurons were significantly diminished in the adult cortex. Interestingly, PV expression in normal rat cortices shows layer-specific age dependency (Hof *et al*, 1999): PV appears in deep layers (V–VI) at P6, in layer IV between P8 and P11, and finally in layers II–III by P21 (Sánchez *et al*, 1992). Thus, it is possible that PV neurons are vulnerable to PCP because at the time of administration these neurons do not yet express PV, but when administered after PV is expressed, the decrease in $[Ca^{2+}]_i$ caused by block of NMDAR could be effectively buffered. A deficit in $[Ca^{2+}]_i$ after NMDAR blockade has been reported in cultured dissociated neurons (Takadera *et al*, 1999; Turner *et al*, 2002) and the role of a $[Ca^{2+}]_i$ deficit in caspase-3 activation after exposure to an MK-801/CNQX combination was confirmed by either reduction of extracellular calcium or the exposure to BAPTA-AM, an intracellular calcium chelator (Yoon *et al*, 2003). Increasing $[Ca^{2+}]_i$ with thapsigargin or ionomycin was able to antagonize MK801-induced death measured 24 h after application (Turner *et al*, 2002). Also, while the current study was in progress, a study appeared that confirmed that a deficit in $[Ca^{2+}]_i$ induced by acute injections of nimodipine (an L-type calcium channel blocker) promoted age-dependent apoptosis in neonatal animals in a manner that was strikingly similar to that found for MK801 (Turner *et al*, 2007). Unlike the traditional concept in which CBPs act as buffers to limit the rise in intracellular free calcium concentration following a toxic stimulus (Baimbridge *et al*, 1992; Chard *et al*, 1993), these results support the hypothesis that CBPs, such as PV, can also protect developing neurons from a deficit in $[Ca^{2+}]_i$ caused by physiological or toxic signals that limit calcium entry. However, this hypothesis does not explain PCP-induced

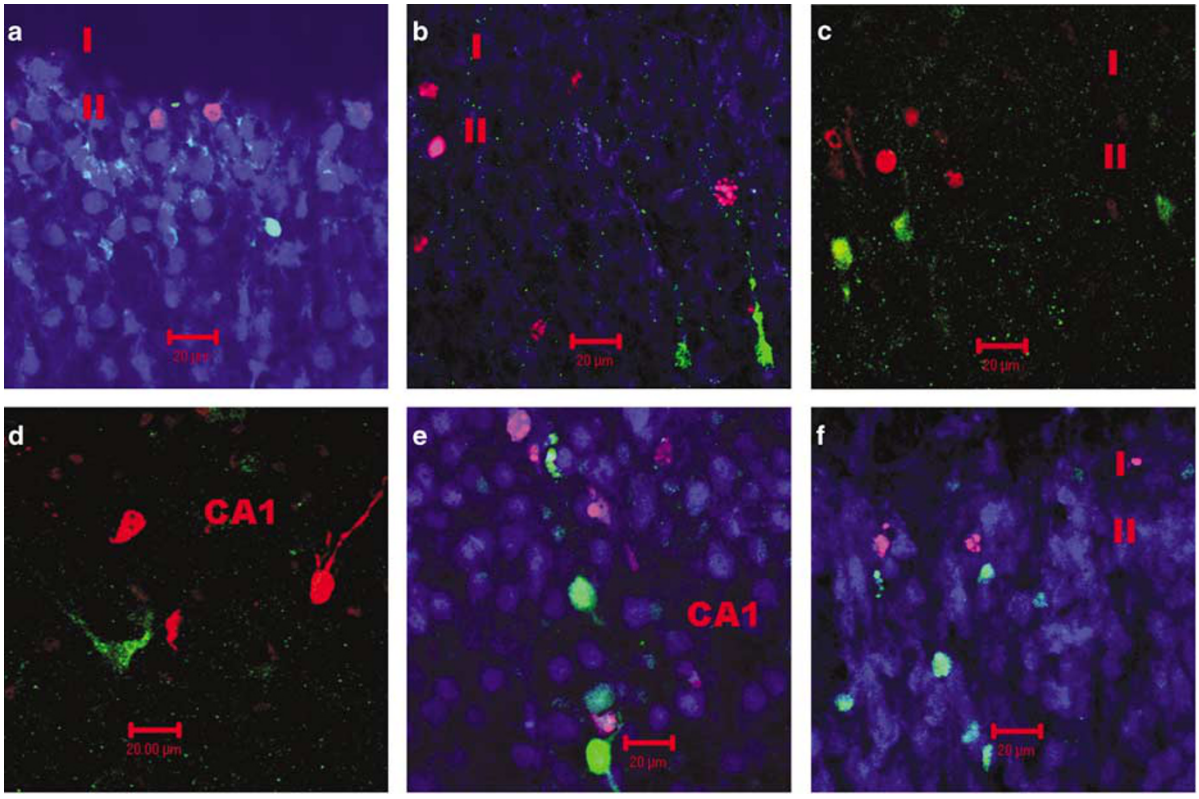

Figure 6 Representative microphotographs showing failure to colocalize apoptotic markers (TUNEL or cleaved caspase-3) with CR or CB in the same neurons in studied brain regions of PND7 rat pups 9 h after PCP (10 mg/kg, s.c.) injection. (a) Motor cortex: CR (green), TUNEL-stained multifragmented nuclei (red) and NeuN (blue, a neuron-specific protein). (b) Cg (cingulate cortex): CR (green), TUNEL (red, multifragmented nuclei), and GFAP (blue, glial fibrillary acidic protein). (c) S1 (primary somatosensory cortex): CR (green), and cleaved caspase-3 (red). (d) Hippocampal CA1 (coronal section): CR (green) and cleaved caspase-3 (red). (e) CA1 (sagittal section): CB (green) and TUNEL-labeled multifragmented nuclei (red) and NeuN (blue). (f) S1: CB (green), TUNEL-positive multifragmented nuclei (red) and NeuN (blue). Scale bars = 20 μm.

neurodegeneration in all of the targeted brain regions during development. For instance, the striatum and hippocampal CA1 regions also showed late PV expression (not present at PND7) as well as PCP-induced neuronal apoptosis at PND7. However, these regions did not exhibit significant PCP-induced deficits of PV-containing neurons in adulthood. Further, following PCP administration, the diminished number and extent of dendritic branches of PV-positive neurons in the lateral CPu suggests a potential protective role for PV expression in this region, but the intact neuronal soma suggests that the PV protection hypothesis in its present form does not completely account for our observations in either this region or the hippocampal CA1 area.

It should be pointed out that subchronic administration of NMDA receptor antagonists to adolescent or adult rodents also has been documented to cause an apparent loss of PV-expressing neurons in various regions, including the hippocampus (Reynolds *et al*, 2004; Keilhoff *et al*, 2004; Rujescu *et al*, 2006), M1 and PFC cortices (Cochran *et al*, 2002, 2003; Abdul-Monim *et al*, 2007), and the dorsal and reticular nucleus of the thalamus (Egerton *et al*, 2005). However, since NMDA receptor antagonists are not neurotoxic in either adolescent or adult rodent brains (Ikonomidou *et al*, 1999), the mechanisms underlying the loss of PV neurons in adults (Sánchez *et al*, 1992; Hof *et al*, 1999) must be distinct from that in early postnatal brains. In the present study, PV-expressing neurons were not present at the time of PCP administration, suggesting that the PV neuron deficit in adults might be a direct neurotoxic effect of PCP on developing neurons. PCP-induced apoptosis was found in brain regions, which showed cell proliferation or neurogenesis simultaneously, but PCP did not target proliferating cells. These data suggest that PCP administration during development might target post-mitotic neurons instead of mitotic cells. Although the targeted neurons probably were born prenatally (Bayer and Altman, 2004) and had finished their migration as evidenced by their distribution in cortical layers 2–4, these neurons might still be immature in ways that are not currently understood.

Although the total neuron numbers in brain regions such as the nuclei of mediodorsal, AV/ AM of thalamus have been reported to be significantly diminished in schizophrenia (Pakkenberg, 1990; Popken *et al*, 2000; Young *et al*, 2000; Byne *et al*, 2002; Danos *et al*, 2003), this disease is not characterized by large-scale neuronal loss (Selemon and Goldman-Rakic, 1999) in any area, especially the cerebral cortex (Pakkenberg, 1993) and hippocampus (Heckers *et al*, 1991; Walker *et al*, 2002). However, cross-sectional and especially longitudinal MRI neuroimaging studies have demonstrated an enlargement of the lateral and third ventricles as well as a reduction of cortical gray matter volume in the whole cortex, especially the PFC and temporal areas (Shenton *et al*, 2001), as well as the hippocampus (Nelson

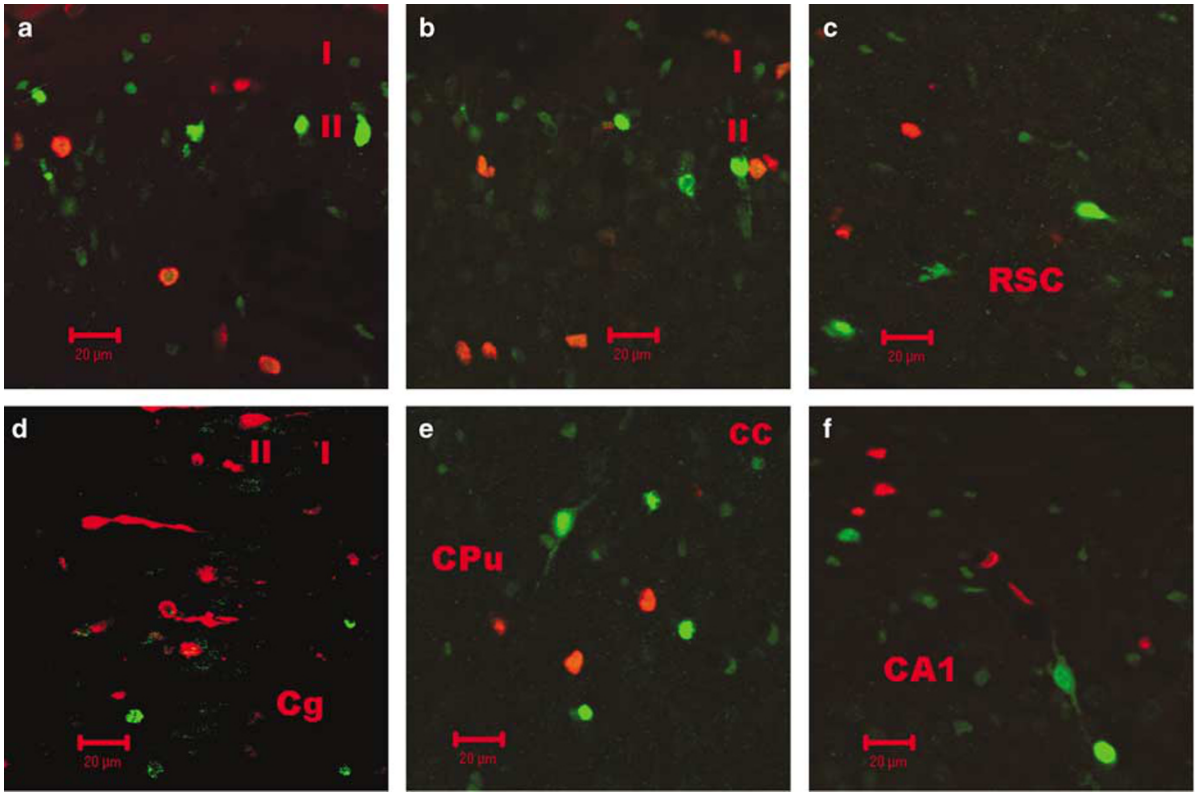

Figure 7 Representative microphotographs showing failure to colocalize BrdU (red) and cleaved caspase-3 (green) in the same neurons of the studied brain regions 9 h after PCP (10 mg/kg) injection at PND7. (a) S1 (primary somatosensory cortex); (b) motor cortex; (c) RSC (retrosplenial cortex); (d) Cg (cingulate cortex): BrdU (green), caspase-3 (red); (e) lateral striatum (CPu); (f) CA1 (coronal section). Scale bars = 20 μm.

et al, 1998). These neuroanatomical abnormalities were found in patients with first-episode schizophrenia (Gur *et al*, 1998; Steen *et al*, 2006), in childhood-onset patients (Thompson *et al*, 2001; Gogtay *et al*, 2004), and in patients who later developed psychosis (Pantelis *et al*, 2003). Although the reduction of cortical gray matter volume might be the result of decreased or shorter dendrites and lack of other subcellular components, the reduction in neuronal cell number such as PV neurons might also contribute. In fact, previous post-mortem studies have consistently reported a significant reduction of GABAergic interneurons (small, nonpyramidal) in layer II of the ACC and PFC cortices of schizophrenic brains (Benes *et al*, 1991, 2001; Benes and Berretta, 2001) and hippocampus (Benes *et al*, 1998). These findings should not be ignored because they indicate possible reductions of specific neuron subpopulations even if there is no large-scale neuronal loss. In further studies focusing on subpopulations of GABAergic interneuron, CR-containing neurons have been consistently reported to be unchanged in any regions of schizophrenic brains (Daviss and Lewis, 1995; Woo *et al*, 1998; Reynolds and Beasley, 2001; Reynolds *et al*, 2001; Eyles *et al*, 2002; Cotter *et al*, 2002; Zhang and Reynolds, 2002; Hashimoto *et al*, 2003). CB-containing neurons have been found to be significantly increased in layers 3 and 5/6 of PFC cortex (areas 9 and 46) (Daviss and Lewis, 1995) or decreased in the same regions (PFC, areas 9 and 46) (Reynolds *et al*, 2001). Others have found no significant difference in either ACC cortex (Cotter *et al*, 2002), PFC (area 46), entorhinal cortex (Reynolds *et al*, 2002), or posterior cingulate cortex (areas 30 and 23) (Wheeler *et al*, 2006). Compared to the controversy concerning CB-containing neurons, a deficit of PV-containing neurons has been more consistently observed in prefrontal cortex (Beasley and Reynolds, 1997; Reynolds and Beasley, 2001; Lewis *et al*, 2001; Reynolds *et al*, 2001, 2002), hippocampus subfields (CA1-4, DG) (Zhang and Reynolds, 2002) and AV of thalamus (Danos *et al*, 1998), although two other studies failed to detect significant deficits of PV-containing neurons in PFC (areas 9 and 46), occipital cortex (area 17) (Woo *et al*, 1997) and ACC cortex (Cotter *et al*, 2002). Overall, the present study demonstrated that early postnatal PCP treatment of rats results in profiles of GABAergic subpopulations in young adults as those observed in post-mortem brain samples from schizophrenics. That is, postnatal phencyclidine administration did not affect CB or CR expression, but selectively induced a loss of cortical PV-containing neurons in adulthood.

The mechanistic basis of the cortex-specific effect of PCP on PV neurons is unknown. It could be argued that the decrease of PV neuron density may represent a decrease in PV gene transcription or protein expression instead of an actual reduction of the number of PV-containing neurons. In this context, it is interesting to note that a significant decrease in PV mRNA expression per neuron without a decrease in the density of PV mRNA-positive neurons has been found in PFC layers III–IV of schizophrenic individuals (Hashimoto *et al*, 2003). Ideally, a morphometric counting of the density of total neurons in the regions studied could answer this question. In preliminary experiments, we

attempted to count neurons, using the neuron-specific marker protein, NeuN. However, this was not possible because of the uncertain counting reliability due to the high density and overlap of stained cells in two-dimensional photographs. Nevertheless, a recent study demonstrated that decreased PV mRNA expression level strongly correlated with a decreased density of GAD67 mRNA-positive neurons in the same schizophrenic individuals (Hashimoto *et al*, 2003), and indicates that GAD67 mRNA expression was markedly reduced in PV-expressing neurons that also had reduced, but still detectable, levels of PV mRNA (Lewis *et al*, 2005). Thus, we propose that even if the PCP-induced deficit in cortical PV neurons represents a reduction in PV expression rather than cell loss, it may also be associated with reduced GABA production and in turn, an impairment of GABA neurotransmission.

Reduced GABAergic neurotransmission between PV-containing interneurons and pyramidal neurons has been proposed to contribute to the cognitive deficits, especially impairments in working memory, one of the clinical features of schizophrenia (Lewis and Gonzalez-Burgos, 2006). Reduced GABAergic neurotransmission could result from either decreased GABA synthesis secondary to reduced mRNA levels for the 67 kDa isoform of glutamic acid decarboxylase (GAD67, encoded by *GAD1*) (Lewis *et al*, 2005) or from a frank deficit in PV neuron number. In cortical regions, such as DLPFC, there are three major subpopulations of GABAergic interneurons: PV-containing chandelier and wide arbor or basket neurons, CB-containing double bouquet (DB), neurogliaform and Martinotti neurons, CR-containing DB, and Cajal–Retzius cells (Condé *et al*, 1994). Among them, only chandelier and wide arbor PV-containing GABAergic interneurons form inhibitory synapses on the axon initial segment and the cell body proximal dendrites of pyramidal neurons. Since the inhibitory synapses are located near the site of action potential generation in pyramidal neurons, the PV neurons are believed to be specialized to regulate the output of pyramidal neurons by providing inhibitory input (Lewis *et al*, 2005). Therefore, reduction of PV-containing interneuron number or/and decrease PV protein expression might be crucial to the cognitive deficits, especially working memory impairment. In the present study, postnatal PCP administration induced a cortical PV neuron deficit, which is consistent with that of a cortical PV deficit in schizophrenic individuals. Thus, the developmental dependence of PCP-induced reduction of PV neurons seen in adult rats may serve as a model with which to explore the pathophysiology of schizophrenia and to search for therapeutic interventions.

ACKNOWLEDGEMENTS

We are grateful to Ms Tiffany E Springsted and Ms Jing Wang for their technical assistance and to Mr Eugene Knutson and Dr Thomas Albrecht, Infectious Disease and Toxicology Optical Imaging Core (IDTOIC), the University of Texas Medical Branch at Galveston, TX, USA for their help with confocal microscopy. This work was supported by grants MH63871 and DA02073 from the US Department of Health and Human Services.

DISCLOSURE/CONFLICT OF INTEREST

The authors declare that, except for income received from their primary employer, no financial support or compensation has been received from any individual or corporate entity over the past 3 years for research or professional service, and there are no personal financial holdings that could be perceived as constituting a potential conflict of interest.

REFERENCES

Abdul-Monim Z, Neill JC, Reynolds GP (2007). Sub-chronic psychotomimetic phencyclidine induces deficits in reversal learning and alterations in parvalbumin-immunoreactive expression in the rat. *J Psychopharmacol* **21**: 198–205.

Abekawa T, Ito K, Nakagawa S, Koyama T (2007). Prenatal exposure to an NMDA receptor antagonist, MK-801 reduces density of parvalbumin-immunoreactive GABAergic neurons in the medial prefrontal cortex and enhances phencyclidine-induced hyperlocomotion but not behavioral sensitization to methamphetamine in postpubertal rats. *Psychopharmacology (Berl)* **192**: 303–316.

Alcántara S, Ferrer I, Soriano E (1993). Postnatal development of parvalbumin and calbindin D28K immunoreactivities in the cerebral cortex of the rat. *Anat Embryol (Berl)* **188**: 63–73.

Alexiades MR, Cepko C (1996). Quantitative analysis of proliferation and cell cycle length during development of the rat retina. *Dev Dyn* **205**: 293–307.

Arnold SE, Hyman BT, Van Hoesen GW, Damasio AR (1991). Some cytoarchitectural abnormalities of the entorhinal cortex in schizophrenia. *Arch Gen Psychiatry* **48**: 625–632.

Baimbridge KG, Celio MR, Rogers JH (1992). Calcium-binding proteins in the nervous system. *TINS* **15**: 303–308.

Bayer SA, Altman J (2004). Chapter 2: development of the telencephalon, neuronal stem cells, neurogenesis, neuronal migration. In: Paxinous G (ed) *The Rat Nervous System*, 3rd edn. Academic Press: San Diego. pp 27–73.

Beasley CL, Reynolds GP (1997). Parvalbumin-immunoreactive neurons are reduced in the prefrontal cortex of schizophrenics. *Schiz Res* **24**: 349–355.

Benes FM, Berretta S (2001). GABAergic interneurons: implications for understanding schizophrenia and bipolar disorder. *Neuropsychopharmacology* **25**: 1–27.

Benes FM, Kwok EW, Vincent SL, Todtenkopf MS (1998). A reduction of nonpyramidal cells in sector CA2 of schizophrenics and manic depressives. *Biol Psychiatry* **44**: 88–97.

Benes FM, McSparren J, Bird ED, SanGiovanni JP, Vincent SL (1991). Deficits in small interneurons in prefrontal and cingulate cortices of schizophrenic and schizoaffective patients. *Arch Gen Psychiatry* **48**: 996–1001.

Benes FM, Vincent SL, Todtenkopf M (2001). The density of pyramidal and nonpyramidal neurons in anterior cingulate cortex of schizophrenic and bipolar subjects. *Biol Psychiatry* **50**: 395–406.

Bhide PG (1996). Cell cycle kinetics in the embryonic mouse corpus striatum. *J Comp Neurol* **374**: 506–522.

Byne W, Buchsbaum MS, Mattiace LA, Hazlett EA, Kemether E, Elhakem SL *et al* (2002). Postmortem assessment of thalamic nuclear volumes in subjects with schizophrenia. *Am J Psychiatry* **159**: 59–65.

Carlsen J, De Olmos JS (1981). A modified cupric-silver technique for the impregnation of degenerating neurons and their processes. *Brain Res* **208**: 426–431.

Chard PS, Bleakman D, Christakos S, Fullmer CS, Miller RJ (1993). Calcium buffering properties of calbindin D28k and parvalbumin in rat sensory neurones. *J Physiol* **472**: 341–357.

Cochran SM, Fujimura M, Morris BJ, Pratt JA (2002). Acute and delayed effects of phencyclidine upon mRNA levels of markers of glutamatergic and GABAergic neurotransmitter function in the rat brain. *Synapse* **46**: 206–214.

Cochran SM, Kennedy M, McKerchar CE, Steward LJ, Pratt JA, Morris BJ (2003). Induction of metabolic hypofunction and neurochemical deficits after chronic intermittent exposure to phencyclidine: differential modulation by antipsychotic drugs. *Neuropsychopharmacology* **28**: 265–275.

Condé F, Lund JS, Jacobowitz DM, Baimbridge KG, Lewis DA (1994). Local circuit neurons immunoreactive for calretinin, calbindin D-28k, or parvalbumin in monkey prefrontal cortex: distribution and morphology. *J Comp Neurol* **341**: 95–116.

Cotter D, Landau S, Beasley C, Stevenson R, Chana G, MacMillan L *et al* (2002). The density and spatial distribution of GABAergic neurons, labelled using calcium binding proteins, in the anterior cingulate cortex in major depressive disorder, bipolar disorder, and schizophrenia. *Biol Psychiatry* **51**: 377–386.

Danos P, Baumann B, Bernstein HG, Franz M, Stauch R, Northoff G *et al* (1998). Schizophrenia and anteroventral thalamic nucleus: selective decrease of parvalbumin-immunoreactive thalamocortical projection neurons. *Psychiatry Res* **82**: 1–10.

Danos P, Baumann B, Krämer A, Bernstein HG, Stauch R, Krell D *et al* (2003). Volumes of association thalamic nuclei in schizophrenia: a postmortem study. *Schizophr Res* **60**: 141–155.

Davidson LL, Heinrichs RW (2003). Quantification of frontal and temporal lobe brain-imaging findings in schizophrenia: a metaanalysis. *Psychiatry Res Neuroimaging* **122**: 69–87.

Daviss SR, Lewis DA (1995). Local circuit neurons of the prefrontal cortex in schizophrenia: selective increase in the density of calbindin-immunoreactive neurons. *Psychiatry Res* **59**: 81–96.

Egerton A, Reid L, McKerchar CE, Morris BJ, Pratt JA (2005). Impairment in perceptual attentional set-shifting following PCP administration: a rodent model of set-shifting deficits in schizophrenia. *Psychopharmacology (Berl)* **179**: 77–84.

Eldridge SR, Tilbury LF, Goldsworthy TL, Butterworth BE (1990). Measurement of chemically induced cell proliferation in rodent liver and kidney: a comparison of 5-bromo-2′-deoxyuridine and [3H]thymidine administered by injection or osmotic pump. *Carcinogenesis* **11**: 2245–2251.

Eyles DW, McGrath JJ, Reynolds GP (2002). Neuronal calcium-binding proteins and schizophrenia. *Schizophr Res* **57**: 27–34.

Falkai P, Schneider-Axmann T, Honer WG (2000). Entorhinal cortex prealpha cell clusters in schizophrenia: quantitative evidence of a developmental abnormality. *Biol Psychiatry* **47**: 937–943.

Fredriksson A, Archer T (2003). Hyperactivity following postnatal NMDA antagonist treatment: reversal by D-amphetamine. *Neurotox Res* **5**: 549–564.

Fredriksson A, Archer T (2004). Neurobehavioural deficits associated with apoptotic neurodegeneration and vulnerability for ADHD. *Neurotox Res* **6**: 435–456.

Fredriksson A, Archer T, Alma H, Gordh T, Eriksson P (2004). Neurofunctional deficits and potentiated apoptosis by neonatal NMDA antagonist administration. *Behav Brain Res* **153**: 367–376.

Gogtay N, Sporn A, Clasen LS, Nugent TF, Greenstein D, Nicolson R *et al* (2004). Comparison of progressive cortical gray matter loss in childhood-onset schizophrenia with that in childhood-onset atypical psychoses. *Arch Gen Psychiatry* **61**: 17–22.

Granato A (2006). Altered organization of cortical interneurons in rats exposed to ethanol during neonatal life. *Brain Res* **1069**: 23–30.

Gritti I, Manns ID, Mainville L, Jones BE (2003). Parvalbumin, calbindin, or calretinin in cortically projecting and GABAergic, cholinergic, or glutamatergic basal forebrain neurons of the rat. *J Comp Neurol* **458**: 11–31.

Gur RE, Cowell P, Turetsky BI, Gallacher F, Cannon T, Bilker W *et al* (1998). A follow-up magnetic resonance imaging study of schizophrenia. Relationship of neuroanatomical changes to clinical and neurobehavioral measures. *Arch Gen Psychiatry* **55**: 145–152.

Harris LW, Sharp T, Gartlon J, Jones DN, Harrison PJ (2003). Long-term behavioural, molecular and morphological effects of neonatal NMDA receptor antagonism. *Eur J Neurosci* **18**: 1706–1710.

Harrison PJ, Weinberger DR (2005). Schizophrenia genes, gene expression, and neuropathology: on the matter of their convergence. *Mol Psychiatry* **10**: 40–68.

Hashimoto T, Volk DW, Eggan SM, Mirnics K, Pierri JN, Sun Z *et al* (2003). Gene expression deficits in a subclass of GABA neurons in the prefrontal cortex of subjects with schizophrenia. *J Neurosci* **23**: 6315–6326.

Hayes NL, Nowakowski RS (2000). Exploiting the dynamics of S-phase tracers in developing brain: interkinetic nuclear migration for cells entering *versus* leaving the S-phase. *Dev Neurosci* **22**: 44–55.

Hayes NL, Nowakowski RS (2002). Dynamics of cell proliferation in the adult dentate gyrus of two inbred strains of mice. *Dev Brain Res* **134**: 77–85.

Heckers S (2001). Neuroimaging studies of the hippocampus in schizophrenia. *Hippocampus* **11**: 520–528.

Heckers S, Heinsen H, Geiger B, Beckmann H (1991). Hippocampal neuron number in schizophrenia. A stereological study. *Arch Gen Psychiatry* **48**: 1002–1008.

Hof PR, Glezer II, Conde F, Flagg RA, Rubin MB, Nimchinsky EA *et al* (1999). Cellular distribution of the calcium-binding proteins parvalbumin, calbindin, and calretinin in the neocortex of mammals: phylogenetic and developmental patterns. *J Chem Neuroanat* **16**: 77–116.

Hoffman PL, Rabe CS, Moses F, Tabakoff B (1989). *N*-methyl-D-aspartate receptors and ethanol: inhibition of calcium flux and cyclic GMP production. *J Neurochem* **52**: 1937–1940.

Ikonomidou C, Bittigau P, Ishimaru M, Wozniak DF, Koch C, Genz K *et al* (2000). Ethanol-induced apoptotic neurodegeneration and fetal alcohol syndrome. *Science* **287**: 1056–1060.

Ikonomidou C, Bosch F, Miksa M, Bittigau P, Vockler J, Dikranian K *et al* (1999). Blockade of NMDA receptors and apoptotic neurodegeneration in the developing brain. *Science* **283**: 70–74.

Jakob H, Beckmann H (1986). Prenatal developmental disturbances in the limbic allocortex in schizophrenics. *J Neural Transm* **65**: 303–326.

Javitt DC, Zukin SR (1991). Recent advances in the phencyclidine model of schizophrenia. *Am J Psychiatry* **148**: 1301–1308.

Keilhoff G, Becker A, Grecksch G, Wolf G, Bernstein HG (2004). Repeated application of ketamine to rats induces changes in the hippocampal expression of parvalbumin, neuronal nitric oxide synthase and cFOS similar to those found in human schizophrenia. *Neuroscience* **126**: 591–598.

Komitova M, Perfilieva E, Mattsson B, Eriksson PS, Johansson BB (2002). Effects of cortical ischemia and postischemic environmental enrichment on hippocampal cell genesis and differentiation in the adult rat. *J Cereb Blood Flow Metab* **22**: 852–860.

Konick LC, Friedman L (2001). Meta-analysis of thalamic size in schizophrenia. *Biol Psychiatry* **49**: 28–38.

Kovalenko S, Bergmann A, Schneider-Axmann T, Ovary I, Majtenyi K, Havas L *et al* (2004). Regio entorhinalis in schizophrenia: more evidence for migrational disturbances and suggestions for a new biological hypothesis. *Pharmacopsychiatry* **36**(Suppl 3): S158–S161.

Kriss JP, Maruyama Y, Tung LA, Bond SB, Revesz L (1963). The fate of 5-bromodeoxyuridine, 5-bromodeoxycytidine, and 5-iododeoxycytidine in man. *Cancer Res* **23**: 260–268.

Lawrie SM, Abukmeil SS (1998). Brain abnormality in schizophrenia—a systematic and quantitative review of volumetric magnetic resonance imaging studies. *Br J Psychiatry* **172**: 110–120.

Lewis DA (2000). GABAergic local circuit neurons and prefrontal dysfunction in schizophrenia. *Brain Res Rev* **31**: 270–276.

Lewis DA, Cruz DA, Melchitzky DS, Pierri JN (2001). Lamina-specific deficits in parvalbuminimmunoreactive varicosities in the prefrontal cortex of subjects with schizophrenia: evidence for fewer projections from the thalamus. *Am J Psychiatry* **158**: 1411–1422.

Lewis DA, Gonzalez-Burgos G (2006). Pathophysiologically based treatment interventions in schizophrenia. *Nat Med* **12**: 1016–1022.

Lewis DA, Hashimoto T, Volk DW (2005). Cortical inhibitory neurons and schizophrenia. *Nat Rev Neurosci* **6**: 312–324.

Lovinger DM, White G, Weight FF (1989). Ethanol inhibits NMDA-activated ion current in hippocampal neurons. *Science* **243**: 1721–1724.

Luby ED, Cohen BD, Rosenbaum G, Gottlieb JS, Kelley R (1959). Study of a new schizophrenomimetic drug; sernyl. *AMA Arch Neurol Psychiatry* **81**: 363–369.

Lynch TP, Cass CE, Paterson AR (1977). Defective transport of thymidine by cultured cells resistant to 5-bromodeoxyuridine. *J Supramol Struct* **6**: 363–374.

Miller MW, Nowakowski RS (1988). Use of bromodeoxyuridine-immunohistochemistry to examine the proliferation, migration and time of origin of cells in the central nervous system. *Brain Res* **457**: 44–52.

Nelson MD, Saykin AJ, Flashman LA, Riordan HJ (1998). Hippocampal volume reduction in schizophrenia as assessed by magnetic resonance imaging: a meta-analytic study. *Arch Gen Psychiatry* **55**: 433–440.

Olney JW, Tenkova T, Dikranian K, Muglia LJ, Jermakowicz WJ, D'Sa C *et al* (2002). Ethanol-induced caspase-3 activation in the *in vivo* developing mouse brain. *Neurobiol Dis* **9**: 205–219.

Packard Jr DS, Menzies RA, Skalko RG (1973). Incorporation of thymidine and its analogue, bromodeoxyuridine, into embryos and maternal tissues of the mouse. *Differentiation* **1**: 397–404.

Pakkenberg B (1990). Pronounced reduction of total neuron number in mediodorsal thalamic nucleus and nucleus accumbens in schizophrenics. *Arch Gen Psychiatry* **47**: 1023–1028.

Pakkenberg B (1993). Total nerve cell number in neocortex in chronic schizophrenics and controls estimated using optical disectors. *Biol Psychiatry* **34**: 768–772.

Palmer TD, Willhoite AR, Gage FH (2000). Vascular niche for adult hippocampal neurogenesis. *J Comp Neurol* **425**: 479–494.

Pantelis C, Velakoulis D, McGorry PD, Wood SJ, Suckling J, Phillips LJ *et al* (2003). Neuroanatomical abnormalities before and after onset of psychosis: a cross-sectional and longitudinal MRI comparison. *Lancet* **361**: 281–288.

Paxinos G, Tork I, Tecott LH, Valentino KL (1994). *Atlas of the Developing Rat Brain*, 2nd edn. Academic Press: New York, USA.

Paxinos G, Watson C (2007). *The Rat Brain in Stereotaxic Coordinates*, 6th edn. Academic Press, Inc.: San Diego, California, USA.

Pearlson GD, Marsh L (1999). Structural brain imaging in schizophrenia: a selective review. *Biol Psychiatry* **46**: 627–649.

Popken GJ, Bunney Jr WE, Potkin SG, Jones EG (2000). Subnucleusspecific loss of neurons in medial thalamus of schizophrenics. *Proc Natl Acad Sci USA* **97**: 9276–9280.

Powell CM, Miyakawa T (2006). Schizophrenia-relevant behavioral testing in rodent models: a uniquely human disorder? *Biol Psychiatry* **59**: 1198–1207.

Reynolds GP, Abdul-Monim Z, Neill JC, Zhang ZJ (2004). Calcium binding protein markers of GABA deficits in schizophrenia—postmortem studies and animal models. *Neurotox Res* **6**: 57–61.

Reynolds GP, Beasley CL (2001). GABAergic neuronal subtypes in the human frontal cortex—development and deficits in schizophrenia. *J Chem Neuroanat* **22**: 95–100.

Reynolds GP, Beasley CL, Zhang ZJ (2002). Understanding the neurotransmitter pathology of schizophrenia: selective deficits of subtypes of cortical GABAergic neurons. *J Neural Transm* **109**: 881–889.

Reynolds GP, Zhang ZJ, Beasley CL (2001). Neurochemical correlates of cortical GABAergic deficits in schizophrenia: selective losses of calcium binding protein immunoreactivity. *Brain Res Bull* **55**: 579–584.

Rujescu D, Bender A, Keck M, Hartmann AM, Ohl F, Raeder H *et al* (2006). A pharmacological model for psychosis based on *N*-methyl-D-aspartate receptor hypofunction: molecular, cellular, functional and behavioral abnormalities. *Biol Psychiatry* **59**: 721–729.

Sadikot AF, Burhan AM, Bélanger MC, Sasseville R (1998). NMDA receptor antagonists influence early development of GABAergic interneurons in the mammalian striatum. *Brain Res Dev Brain Res* **105**: 35–42.

Sánchez MP, Frassoni C, Alvarez-Bolado G, Spreafico R, Fairén A (1992). Distribution of calbindin and parvalbumin in the developing somatosensory cortex and its primordium in the rat: an immunocytochemical study. *J Neurocytol* **21**: 717–736.

Scallet AC, Schmued LC, Slikker W, Grunberg N, Faustino PJ, Davis H *et al* (2004). Developmental neurotoxicity of ketamine: morphometric confirmation, exposure parameters, and multiple fluorescent labeling of apoptotic neurons. *Toxicol Sci* **81**: 364–370.

Selemon LD, Goldman-Rakic PS (1999). The reduced neuropil hypothesis: a circuit based model of schizophrenia. *Biol Psychiatry* **45**: 17–25.

Shenton ME, Dickey CC, Frumin M, McCarley RW (2001). A review of MRI findings in schizophrenia. *Schizophr Res* **49**: 1–52.

Sherwood NM, Timiras PS (1970). *A Stereotaxic Atlas of the Developing Rat Brain*. University of California Press: Berkeley, CA, USA.

Solbach S, Celio MR (1991). Ontogeny of the calcium binding protein parvalbumin in the rat nervous system. *Anat Embryol (Berl)* **184**: 103–124.

Spector R, Berlinger WG (1982). Localization and mechanism of thymidine transport in the central nervous system. *J Neurochem* **39**: 837–841.

Steen RG, Mull C, McClure R, Hamer RM, Lieberman JA (2006). Brain volume in first-episode schizophrenia: systematic review and meta-analysis of magnetic resonance imaging studies. *Br J Psychiatry* **188**: 510–518.

Takadera T, Matsuda I, Ohyashiki T (1999). Apoptotic cell death and caspase-3 activation induced by *N*-methyl-D-aspartate receptor antagonists and their prevention by insulin-like growth factor I. *J Neurochem* **73**: 548–556.

Takahashi T, Nowakowski RS, Caviness Jr VS (1992). BUdR as an S-phase marker for quantitative studies of cytokinetic behaviour in the murine cerebral ventricular zone. *J Neurocytol* **21**: 185–197.

Takahashi T, Nowakowski RS, Caviness Jr VS (1995). The cell cycle of the pseudostratified ventricular epithelium of the embryonic murine cerebral wall. *J Neurosci* **15**: 6046–6057.

Taupin P (2007). BrdU immunohistochemistry for studying adult neurogenesis: paradigms, pitfalls, limitations, and validation. *Brain Res Rev* **53**: 198–214.

Thomas née Williams SA, Segal MB (1996). Identification of a saturable uptake system for deoxyribonucleosides at the blood–brain and blood-cerebrospinal fluid barriers. *Brain Res* **741**: 230–239.

Thomas SA, Davson H, Segal MB (1997). Quantification of efflux into the blood and brain of intraventricularly perfused [3H]-thymidine in the anaesthetized rabbit. *Exp Physiol* **82**: 139–148.

Thompson PM, Vidal C, Giedd JN, Gochman P, Blumenthal J, Nicolson R *et al* (2001). Mapping adolescent brain change reveals dynamic wave of accelerated gray matter loss in very early-onset schizophrenia. *Proc Natl Acad Sci USA* **98**: 11650–11655.

Turner CP, Miller R, Smith C, Brown L, Blackstone K, Dunham SR *et al* (2007). Widespread neonatal brain damage following calcium channel blockade. *Dev Neurosci* **29**: 213–231.

Turner CP, Pulciani D, Rivkees SA (2002). Reduction in intracellular calcium levels induces injury in developing neurons. *Exp Neurol* **178**: 21–32.

Walker MA, Highley JR, Esiri MM, McDonald B, Roberts HC, Evans SP *et al* (2002). Estimated neuronal populations and volumes of the hippocampus and its subfields in schizophrenia. *Am J Psychiatry* **159**: 821–828.

Wang CZ, Johnson KM (2005). Differential effects of acute and subchronic administration on phencyclidine-induced neurodegeneration in the postnatal rat. *J Neurosci Res* **81**: 284–292.

Wang CZ, Johnson KM (2007). The role of caspase-3 activation in phencyclidine-induced neuronal death in postnatal rats. *Neuropsychopharmacology* **32**: 1178–1194.

West MJ (1993). New stereological methods for counting neurons. *Neurobiol Aging* **14**: 275–285.

Wheeler DG, Dixon G, Harper CG (2006). No differences in calcium-binding protein immunoreactivity in the posterior cingulate and visual cortex: schizophrenia and controls. *Prog Neuropsychopharmacol Biol Psychiatry* **30**: 630–639.

Woo TU, Miller JL, Lewis DA (1997). Schizophrenia and the parvalbumin-containing class of cortical local circuit neurons. *Am J Psychiatry* **154**: 1013–1015.

Woo TU, Whitehead RE, Melchitzky DS, Lewis DA (1998). A subclass of prefrontal gamma-aminobutyric acid axon terminals are selectively altered in schizophrenia. *Proc Natl Acad Sci USA* **95**: 5341–5346.

Wozniak DF, Hartman RE, Boyle MP, Vogt SK, Brooks AR, Tenkova T *et al* (2004). Apoptotic neurodegeneration induced by ethanol in neonatal mice is associated with profound learning/memory deficits in juveniles followed by progressive functional recovery in adults. *Neurobiol Dis* **17**: 403–414.

Wright IC, Rabe-Hesketh S, Woodruff PWR, David AS, Murray RM, Bullmore ET (2000). Meta-analysis of regional brain volumes in schizophrenia. *Am J Psychiatry* **157**: 16–25.

Yoon WJ, Won SJ, Ryu BR, Gwag BJ (2003). Blockade of ionotropic glutamate receptors produces neuronal apoptosis through the Bax-cytochrome C-caspase pathway: the causative role of Ca2+ deficiency. *J Neurochem* **85**: 525–533.

Young C, Jevtovic-Todorovic V, Qin YQ, Tenkova T, Wang H, Labruyere J *et al* (2005). Potential of ketamine and midazolam, individually or in combination, to induce apoptotic neurodegeneration in the infant mouse brain. *Br J Pharmacol* **146**: 189–197.

Young KA, Manaye KF, Liang CL, Hicks PB, German DC (2000). Reduced number of mediodorsal and anterior thalamic neurons in schizophrenia. *Biol Psychiatry* **47**: 944–953.

Zhang ZJ, Reynolds GP (2002). A selective decrease in the relative density of parvalbumin-immunoreactive neurons in the hippocampus in schizophrenia. *Schiz Res* **55**: 1–10.